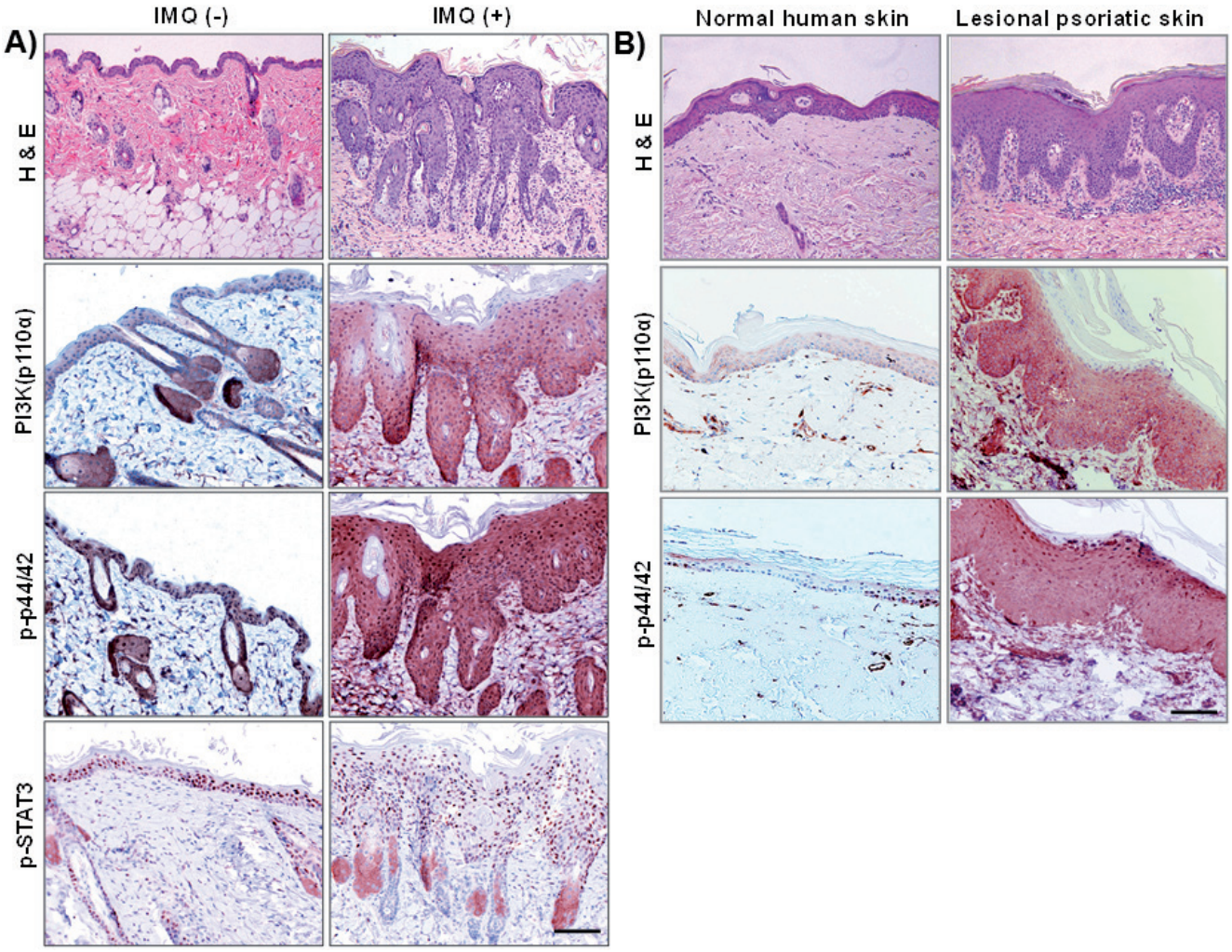

Fig. S1. H & E and immunohistochemical images of control IMQ(-) vs IMQ-treated IMQ(+) Balb/c mouse skin sections(A and C) and human control and lesional psoriatic skin (B and C). Images show activation of (A and B) PI3K, P44/42 and Stat3 upon pretreatment of mice skin with IMQ (+) compared with control IMQ (–) and upregulation of these markers in psoriatic skin lesions compared to normal skin. Staining of phospho-p44/42 (Thr^{202}/Try^{204}). Scale Bar =50μm. (C) High power magnification of a sections of PPAR β/δ staining of inflamed psoriatic skin lesion (top 2 images) and IMQ-induced Balb/c mice skin lesions(bottom 2 images) Prominently intense PPAR β/δ staining can be seen in the entire lesional epidermis of both human psoriasis and IMQ-induced psoriasiform dermatitis skin. From the basal to spinous layers the staining was mostly cytoplasmic with few cells showing nuclear staining. Very strong nuclear and cytoplasmic staining was observed through the differentiating compartments (Inset 150 μm). By contrast in normal skin very week cytoplasmic staining of PPAR β/δ and occasional nuclear staining was observed in the stratum granulosum. Additionally, a strong expression pattern was observed in IMQ-induced Balb/c mouse lesions. There was strong involvement of hair follicle and the entire epithelium showed both nuclear and cytoplasmic staining (top panel), compared to weak punctate suprabasal nuclear expression in control Balb/c mouse skin (bottom panel; inset 150 μm).

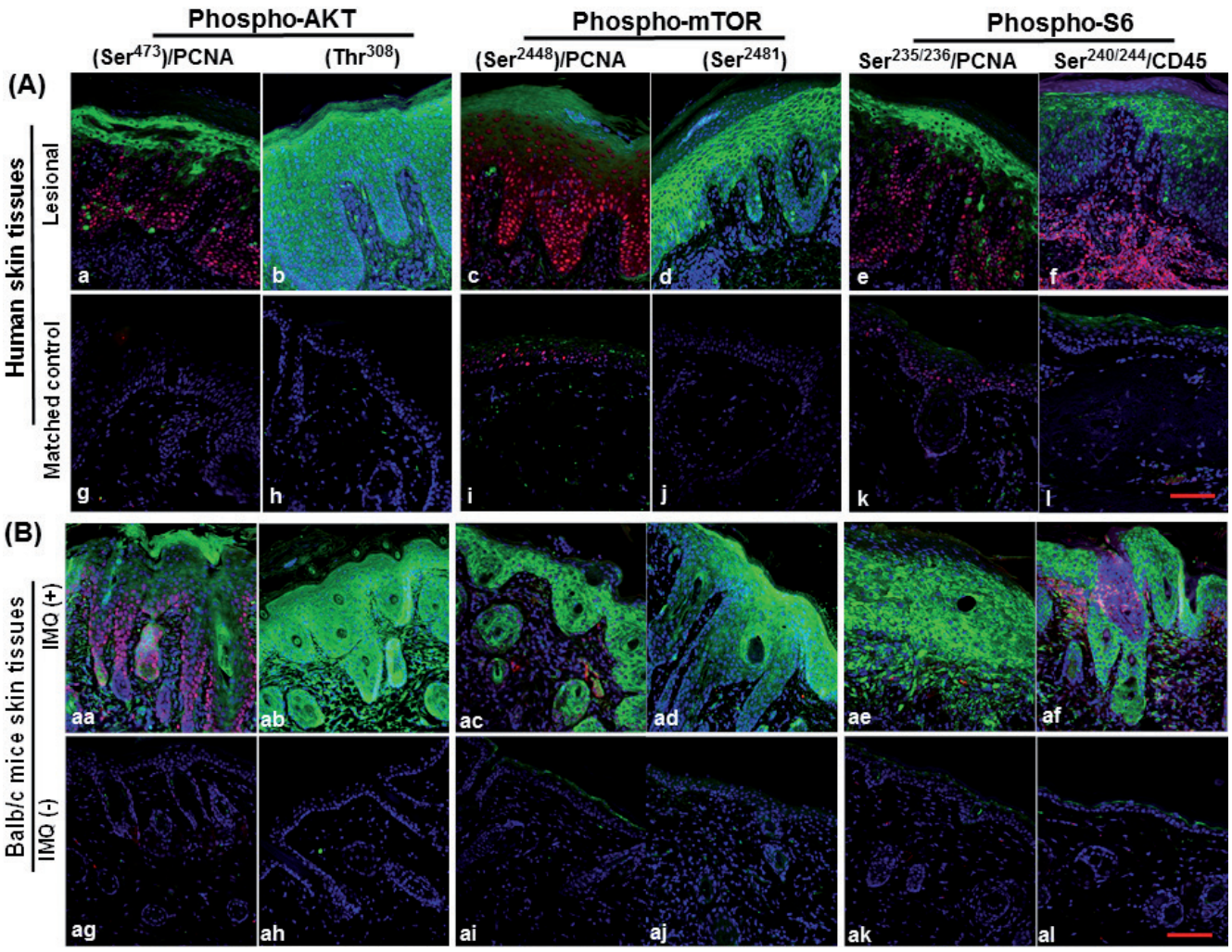

Fig. S2. Double immunofluorescence images of human psoriatic vs healthy skin(A), and IMQ-treated vs control Balb/c mouse skin sections(B). Images show differential phosphorylation of Akt(Ser^{473}/Thr^{308})(a,b)/(g,h) and (aa,ab)/(ag,ah), mTOR(Ser^{2448} and Ser^{2481})(c,d)/(i,j) and (ac,ad)/(ai,aj), S6($Ser^{235/236}$/$Ser^{240/244}$)(e,k)/ (f–l) and (ae–ak)/(af–al) in human and mice respectively stained green. PCNA-and-CD45 positive cells in red. In normal human and Balb/c mouse skin (g,l) and (gl,l1), phospho-Akt(Ser^{473}/Thr^{308}) was completely absent whereas phospho-mTOR($Ser^{2448/2481}$) and phospho-S6($Ser^{235/236}$ and $Ser^{240/244}$) was extremely weak and restricted to the stratum granulosum. In contrast, psoriatic lesions also revealed Akt, mTOR (mostly Ser^{2481}) and phospho-S6 in suprabasal cell layers (a,f) and in IMQ-induced Balb/c mouse lesions (a1,f1) all proteins were over expressed in the entire epidermis. All samples were stained blue with DAPI. Scale bars =50 μm.

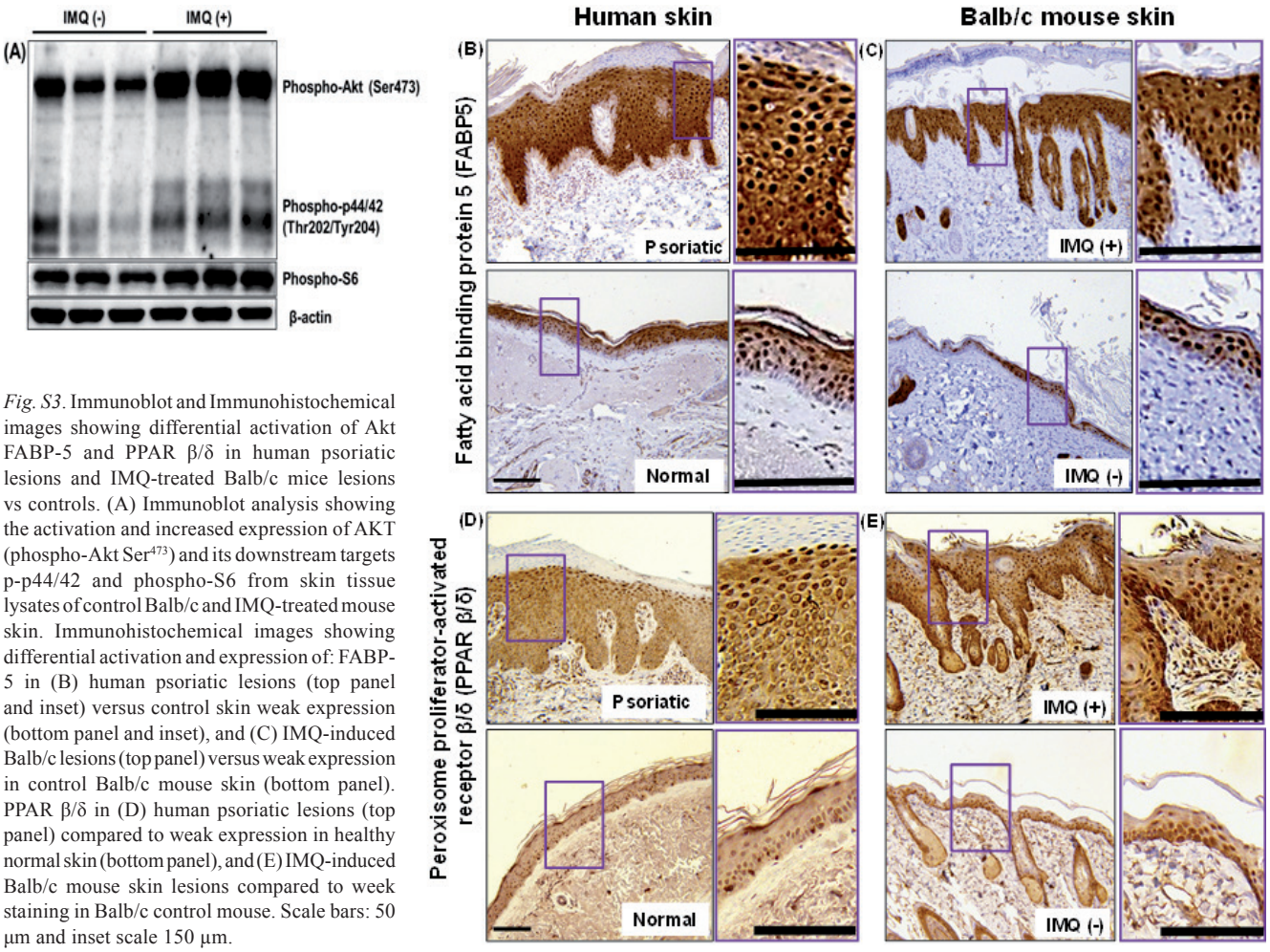

Fig. S3. Immunoblot and Immunohistochemical images showing differential activation of Akt FABP-5 and PPAR β/δ in human psoriatic lesions and IMQ-treated Balb/c mice lesions vs controls. (A) Immunoblot analysis showing the activation and increased expression of AKT (phospho-Akt Ser^{473}) and its downstream targets p-p44/42 and phospho-S6 from skin tissue lysates of control Balb/c and IMQ-treated mouse skin. Immunohistochemical images showing differential activation and expression of: FABP-5 in (B) human psoriatic lesions (top panel and inset) versus control skin weak expression (bottom panel and inset), and (C) IMQ-induced Balb/c lesions (top panel) versus weak expression in control Balb/c mouse skin (bottom panel). PPAR β/δ in (D) human psoriatic lesions (top panel) compared to weak expression in healthy normal skin (bottom panel), and (E) IMQ-induced Balb/c mouse skin lesions compared to week staining in Balb/c control mouse. Scale bars: 50 μm and inset scale 150 μm.

Appendix S1

SUPPLEMENTARY MATERIALS

Ethical consideration

Human subject study was approved by the Scientific and IRB ethics committee of the School of Medicine and Public Health (SMPH), University of Wisconsin (UW)-Madison and studies were performed following the Declaration of Helsinki protocols. All animal experiments were performed in compliance with the School of Medicine and Public Health (SMPH) Institutional Animal Care and Use Committee (IACUC) guidelines and protocols were approved by the Animal Care and Use Committee at the University of Wisconsin-Madison (Madison, WI).

Mice and IMQ-induce murine psoriasis-like skin model: Six –to-eight-week-old male Balb/c mice from Harlan laboratories (Madison, WI) were used. After arrival, mice were acclimatized for 1 week before commencing the experiments, and were maintained under standard pathogen-free conditions: temperature of 24 ± 2°C, relative humidity of 50 ± 10% and 12 h room light/12 h dark cycle, and fed Purina Chow diet and water ad libitum. The dorsal surface of Balb/c mice were shaved with electrical clippers and residual hair cleared with Nair, and mice were allowed to rest for 48 hours before all experiments. Mice received daily topical dose of 62.5 mg of commercially available IMQ cream (5%) (Aldara, 3M Pharmaceuticals), on the shaved back for 5 days, and received the same booster dose for 9 consecutive days to achieve optimal chronic inflammation. For controls, mice received Vaseline, since the IMQ vehicle has been shown to induce inflammatory responses (S1). All IMQ-treated ($n = 6$) and pair-matched control ($n = 6$) mouse skin were freshly harvested as earlier described (11), for histological and biochemical analyses.

Patients and healthy human tissue collection. Thin cuts; 6-µm cryo-sections or 5-µm paraffin sections were obtained from all analyzed human lesional psoriatic and pair-matched healthy skin. Retrospective lesional skin samples were from untreated patients with active untreated psoriasis ($n = 12$) including different clinical grades mild, moderate and severe plaque-type, and fresh healthy skin ($n = 10$) taken after written informed consent.

Histology, immunohistochemistry and immunofluorescence. Paraffin embedded and frozen cryo-sections from inflamed psoriatic, IMQ-induced mouse skin lesions and their respective matched control skin tissues were processed for histology and immunostaining as previously described (S2, S3)). Briefly, paraffin embedded samples were de-paraffinized, heated and pretreated at 95°C for 50 min in 10 mmol L−1 sodium citrate (pH 6·0) in a Steamer set at 120V (IHCWORLD, LLC, Life Science). Frozen sections were fixed in acetone and permeabilized with TBS-T [50 mmol L−1 Tris–HCl (pH 7·5), 150 mmol L−1 NaCl, 0·3% Triton X-100]. For immunofluorescence (IF), all specimens were blocked with 10% normal goat serum (NGS)/2% bovine serum albumin (BSA) dissolved in TBS-T for 30 min whereas, sections stained by immunohischemistry (IHC) were blocked in 5% NGS/horse serum/2% BSA in TBS-T for 1hr at room temperature (RT) and incubated overnight at 4°C with the following primary or isotype controls antibodies. The antibodies used were; rabbit anti-phospho-Akt (Ser473(1:250, #4060; Thr308(1:200;#13038)), rabbit anti-phospho-mTOR (Ser2448(D9C2) (1:200, #5536)), rabbit antiphospho-S6(Ser235/236) (1:400; #2211); rabbit anti-phospho-S6(Ser240/244) (1:400; #2215); rabbit anti-PI3 Kinase (p110α (C73F8) (1:200; # 4249); rabbit anti-P-p44/42(Thr202/Tyr204) (1:200; # 4370) and rabbit antiPhospho-Stat3 (Tyr705) (1:200; #9145) all from (Cell Signaling, Danvers, MA); rabbit anti-phospho-mTOR (Ser2481(1:200, # ab45996) from abcam; mouse antiphospho-S6(Ser240) (1:100; DAKO #M7300); rabbit anti-PCNA (1:200; DAKO #A0067); mouse anti-CD45 (1:100; DAKO #M0701), rabbit anti-PPARβ/δ (1:200: #NBP1-39684, Novus Biologicals), rat anti-mCD45(1:200: # MAB114; R&D Systems); rabbit anti-FABP5 (1:200: # 12348-1AP ProteinTech Group) and anti-hFABP5 (1:200: # AF3077, R&D Systems). After washing, IF samples were incubated for 1 h with Alexa Fluor 488 or Alexa Fluor 594 HRP-conjugated secondary antibodies (1: 600; Invitrogen), and following several washes were mounted with Prolonged® Gold Anti-fade reagent containing 4′,6-diamidino-2-phenylindole (DAPI; Invitrogen). IHC stained samples were processed as described earlier (S2, S3). Images were generated using the Nuance® EX/FX and Vectra™ (PerkinElmer, Boston, MA) multiplexing image technology platform and analyzed by the inForm software. Control immunostaining utilizing mouse melanoma tumor treated with dual mTOR inhibitor (fisetin) or placebo confirmed the phospho-S6 antibodies are highly specific for Akt/mTOR-regulated phosphorylation sites. Control sections were prepared following incubation with the appropriate isotype control mAb or following addition of biotinylated mAb conjugate or secondary conjugated antibody alone.

Preparation of tissue lysates and Western Blot analysis. Mouse skin biopsied tissues were lysed, homogenized, ultra-sonicated in ice-cold Cell Lysis Buffer (affymetrix, eBioscience, # EPX-99999-000) freshly supplemented with 1mM PMSF and protease inhibitor cocktail Set III (Calbiochem). The lysates were quantified and normalized as earlier described (S2, 8). Thirty microgram (30 µg) of each protein sample was subjected to SDS 12% polyacrylamide gel electrophoresis (PAGE) and blotted onto nitrocellulose membranes. After 45 min blocking in 5% nonfat dry milk in TBS-T, membranes were probed with the indicated PathScan® Multiplex Western Cocktail I (1:200; #5301) antibody (Cell Signaling, Danvers, MA) overnight at 4°C. Samples were incubated for 1hr with horse-radish peroxidase-conjugated anti-rabbit or anti-mouse secondary antibodies (Cell Signaling Technology or Pierce/Thermo Fischer Scientific), developed with ECL (GE Healthcare) and Super Signal West Femto chemiluminescent substrate (Pierce/Thermo Fischer Scientific) and visualized using an automatic imager (Bio Rad) as described (8).

SUPPLEMENTARY REFERENCES

S1. Flutter B, Nestle FO. TLRs to cytokines: mechanistic insights from the imiquimod mouse model of psoriasis. Eur J Immunol 2013; 43: 3138–3146.

S2. Chamcheu JC1, Pal HC, Siddiqui IA, Adhami VM, Ayehunie S, Boylan BT, et al. Prodifferentiation, anti-inflammatory and antiproliferative effects of delphinidin, a dietary anthocyanidin, in a full-thickness three-dimensional reconstituted human skin model of psoriasis. Skin Pharmacol Physiol 2015; 28: 177–188.

S3. Chamcheu JC, Afaq F, Syed DN, Siddiqui IA, Adhami VM, Khan N, et al. Delphinidin, a dietary antioxidant, induces human epidermal keratinocyte differentiation but not apoptosis: studies in submerged and three-dimensional epidermal equivalent models. Exp Dermatol 2013; 22: 342–348.